Інструмент, порошки, пасти

Y. Chen[1, 2,*], X. Chen[3], L. AlOuarab[3], T. Opoz[3], X. P. Xu[2], G. Yu[4]

[1]College of Mechanical Engineering and Automation, Huaqiao University, Xiamen, PR China

[2]Ministry of Education Engineering Research Center for Brittle Materials Machining, Huaqiao University, Xiamen, PR China

[3]Faculty of Engineering and Technology, Liverpool John Moores University, Liverpool, UK

[4]Roll forging institute, Jilin University, Changchun, PR China

42371502@qq.com

Morphology analysis and characteristics evaluation of typical super abrasive grits in micron scale

Distribution characterization of geometry shape and size of abrasive grits with high quality in tight size band and exact pattern is crucial for modern tool manufacturer to make fine powder abrasive tool and other powder tools, but complex to be classified and evaluated accurately due to the lack of scientific method. In contrast to industrial methods with sieving mesh size or simplified projection criteria with circumscribed (inscribed or escribed) circle or rectangle, a set of new systemic criteria is developed and validated by measuring three representative grits samples in micron scale under 2D/3D microscopy platform. The features of micron abrasive grits under morphology classification include total four groups, six sub-groups and eighteen sub-types in consideration of spatial geometry and statistical size distribution. For grinding performance analysis and simulation, it would be better to use a set of dominant volumetric geometries rather than use single simple geometry. Furthermore, the significance of abrasive grits geometries in grinding performance is discussed.

Keywords: *super abrasive grit, morphology analysis, characteristics categorization, microscopy technique, size distribution.*

INTRODUCTION

Morphology knowledge on characteristics and distribution of geometry shape and size of abrasive grit is a prerequisite for abrasive tool producers, researchers and users to analyse and improve grinding performance. In grinding, the main task of abrasive grits characterised by size, shape stochastic distribution and other mechanical-thermal properties is to conduct either material removal by

forming chip in ductile material or surface shattering in brittle material [1–4]. Thus not only morphological but also physicochemical properties of abrasive grits, together with abrasive tool preparation and grinding conditions, are crucial to achieve better ground surface, dimensional tolerance and process stability.

In many previous researches on grinding dynamics, the shapes of abrasive grits are commonly assumed to be either individual cone or pyramid with designated angles, even simplest sphere, or ellipsoid [1, 3, 5, 6] for solid grit modelling and grinding simulation to analyse elastic-plastic deformation and stress-strain distribution in material removal. In fact, the actual grits distributed on the circumference of abrasive tool are not exactly same even far away from aforementioned geometrical assumption in grinding. As a result, the conclusions drawn from scratching tests utilizing single grit or multiple grits with predefined and simplified geometrical shape do not convince very well and the grinding behaviour in the grit-material contact zone can hardly be elaborated with satisfied accuracy.

To determine morphology distribution of abrasive grits, electrical sensing zone, forward and right angle light scattering, dynamic light scattering, centrifugal sedimentation and automated image analysis (optical or scanning electron microscope (SEM)) are used widely in industry by implementing two-dimension similarity criteria of regular shapes projection [7–9]. Some facilities, such as particle size analyzers, are currently available for the determination of size distribution of subsieve diamond and cubic boron nitride (CBN) powders [10–13]. However until now, the studies find that no single measurement apparatus and no relative three-dimension evaluation criteria are available to determine all information on grit quality, property and performance.

With the development of special market demands of designated grits, abrasive tool producers are facing challenges driven by customers, which requires new generation of tool products with optimized morphology and strict size distribution in micron scales. In order to investigate ideal material removal mechanism for better grinding behaviour and ground surface quality, highly-engineered abrasive tools are manufactured with specially defined grit pattern or with micro-cutting edges, i.e. with controlled size, required shape and distribution on surface of abrasive tools [14–17]. Due to aforementioned extraordinary uncertainty and dissimilarity of randomly distribution or irregularly abrasive shapes, there are few procedures and criteria on abrasive assessment and classification published. This paper attempts to comprehensively expound a more feasible procedure on identifying spatially volumetric geometrical characteristics with high accuracy (i.e. how close a measured value is to the true value), precision (i.e. the variation in repeated measurements conducted by same device and operator) and size distribution of micron grits in microscopy assessment. A set of newly presentd systemic criteria of morphology categorization are proposed to define dominant morphological characteristics of the grits with mathematic statistical methods, which will benefit core competency of stakeholders, such as abrasive grit producers, grinding tool users and researchers for grinding dynamics analysis using finite element method (FEM) simulation and experimental technique. Furthermore, the presented microscopy technique, categorization criteria and 3D abrasive morphological distribution definition could provide a good guidance for abrasive tool manufacturers and users to appraise pre-process quality of abrasive grits and to predict their grinding performance.

SAMPLE MEASUREMENT PRINCIPLE

In practical application, a series of pre-processing procedures in accordance with international standard, including milling and grading, acid cleaning, sieving,

sedimentation, washing and drying, blending, quality controlling etc, are selectively implemented in terms of specific demands of product specification and properties [18]. In the paper, the focus is on geometrical characteristics.

Sieving process

Sieving is a regular process performed easily either by manual work or by machine to separate abrasive grits from uniform sieves in different mesh size grades. Coarse abrasive grits are definitely classified in terms of sieving mesh size. Finer or powder grits are classified by sedimentation process in terms of multiple national and international standards, such as ANSI, FEPA, FEPA, GB/T ISO, etc. [19].

In measurement test, it is noted that determining a grit dimension by means of sieving mesh size does not imply an accurate value, but rather a size band. The band is definitized by means of a set of sieving instruments retaining or passing a number of grits with specific size. However, the quality of sieving process with the physical method largely depends on the shape features of the grits. For example, for the grits in shape of round or bulky cube and triangle, mesh size defines their approximate diameter or circumference, but for the grits in irregular shape (e.g. in needle or spike shape), the maximum dimension of the analyte might be larger than the mesh size as the grits could pass through sieves with their smallest cross-section profile. Therefore, wider size distribution of irregular grits is, higher uncertainty of shape distribution of the grits increases.

Sample preparation process

In sample preparation process, well-dispersed, rather than clusters or over-lapped samples sprayed on the glass slide are needed to avoid difficult-to-capture situation and to carry out microscopy observation tests. In the study, three types of representative samples that have great grinding performance and physical properties with higher hardness, excellent mechanical-thermal properties and highest occupation rate of industrial market worldwide, namely A (coarse diamond grit), B (finer CBN micron grit) and C (finer diamond grit) are listed in Table 1.

Table 1. Specification and properties of the samples

Sample types	Geometry properties	ANSI grain size, µm, and standards (ANSI-B74-16)	Physical properties
A (diamond)	Coarse and dark Sharp polygon edges	302–456; 40/50#	Irregular monocrystal Moderate strength Resin bond
B (CBN)	Finer and dark brown Sharp triangle edges	127–165; 100/120#	Complete crystal form High strength High thermal stability Resin bond
C (diamond)	Powder and light grey Concentrated size distribution	12–22; 9#	Uniform lump microstructure High thermal stability Metal bond

Due to different size magnitudes of three types of samples, a large number of the particles are composed in even just one carat of the samples. The number of the sampled particles observed in tests is only very small proportion of the whole samples. Thus, proper sampling density in tests is crucial to fulfil statistical analyse (i.e. to improve the objectivity of the classification). To eliminate the subjectivity of decision made by the operator, each test is conducted with at least 2–3 independent groups of the samples. Each group of the samples is composed of over 50 particles randomly-captured under an optical microscopy vision area.

Microscopy measurement process

Optical microscopy technique is commonly used to measure sub-sieve powder diamond grits and micron CBN grits by capturing their clear images. The samples in the images are then dimensioned for size analysis and shape classification by means of accessional image software. The process allows the operator to observe the positioned samples and to evaluate their shape characteristics and size band. In general, the sample size is defined as the diameter of minimum circumscribed circle that completely encloses the 2D projected image of the sample (i.e. equivalent circle diameter) or recorded with the longest single dimension of grit edges (LSD) [12].

Prior to measurement, the scale calibration of microscopy device is essential to significantly assure reliability of the test according to accuracy standard and size distribution of the samples. The purpose of scale calibration is to establish a unified metric basis for dimensioning size of the samples in sub-sieve accurately. After that, different size distribution of the samples could be constructed by visually classifying and accumulating counts in sequence. Following such a defined procedure, the characterization criteria of size and shape distribution is elaborated in next section.

So far, automated optical scanning system (e.g. using optical or SEM microscope coupled with a computerized image analyzer) can eliminate most of the fatiguing measurement works [13]. However besides high cost, not a single technique or feasible device is available to measure and identify the size and shape spectrum of the particles at consistent accuracy. Each technique/device is capable of providing optimal application in a certain size range based on specific 2D profile similarity (e.g. circularity and sphericity) characterization.

In the investigation, the images of the particles are captured under a Leica DFC 295/CH9435 optical microscope (Leica Microsystem Ltd, Germany) [20] coupled with an objective lens of magnification 100×, 50×, 20×, 10×, 5×. The microscope, which scanning distance from 0.5 μm to 2000 μm is equipped with a digital camera OLYMPUS BX51M. The size and morphology analysis are carried out with an image analysis software (LAS V3.6). The images of particles are shown in Fig. 1 (sample group A, magnification 5×, scale calibration: 200 μm), Fig. 2 (sample group B, magnification 20×, scale calibration: 125 μm) and Fig. 3 (sample group C, magnification 10×, scale calibration: 10 μm).

In Fig. 1, it is clearly shown that there are many truncated particles with smooth top-surfaces (Area S_1) formed due to natural crystalline fracture in previous milling process. Similar situation is observed from a few of CBN particles in Fig. 2 and some diamond particles in Fig. 3. In contrast to commonly blunt flanks of the particles in Fig. 1 and Fig. 3, sharper flanks of the particle exist in Fig. 2. Further, all length dimensions of the samples edges both at top-surface (Area S_1) and at bottom-surface (Area S_2) in planar shapes of triangle, quadrilateral, pentagon or hexagon, are measured clockwise according to calibrated scale and incrementally

recorded with Origin 8.0 software. Meanwhile for the samples in shape of polygon, maximum size and minimum size between longest single dimension of edges (LSD) and relative dimension of vertical line from the farthest vertex away from LSD are depicted as length (L) and width (W) of the grit only at bottom projection surface (Area S_2) in accordance with sieving mesh size. The length (L) and width (W) of the samples in shape of rhomb or ellipse correspond to major axis and minor axis. By substituting the edges dimensions into quantitative area formulas in Origin 8.0 software, projection areas of the samples, including truncated-surface area (Area S_1) and bottom profile area (Area S_2) and length (L) and width (W) of the grits are obtained and dimensioned in Fig. 1, *b*, Fig. 2, *b*, Fig. 3, *b*. For most particles in Fig. 2, *b* and Fig. 3, *b*, Area S_2 almost overlaps with Area S_1. The aspect ratio (AR) of width to length of each grit is calculated automatically as an important variable to assess shape features.
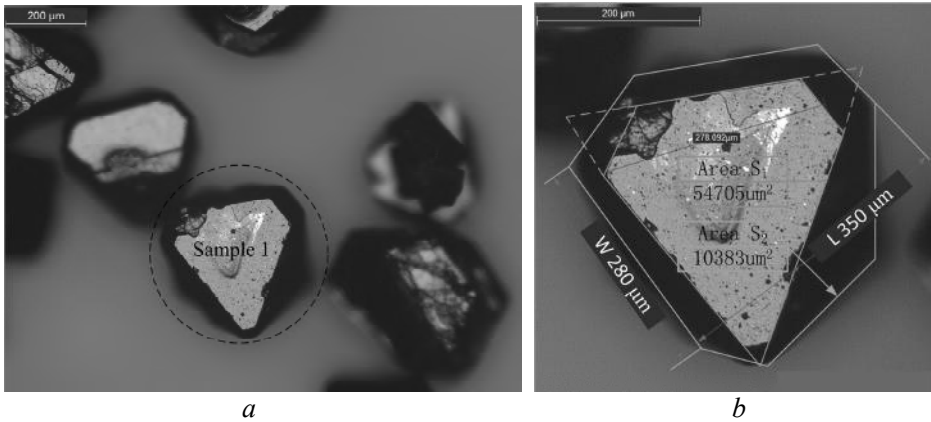

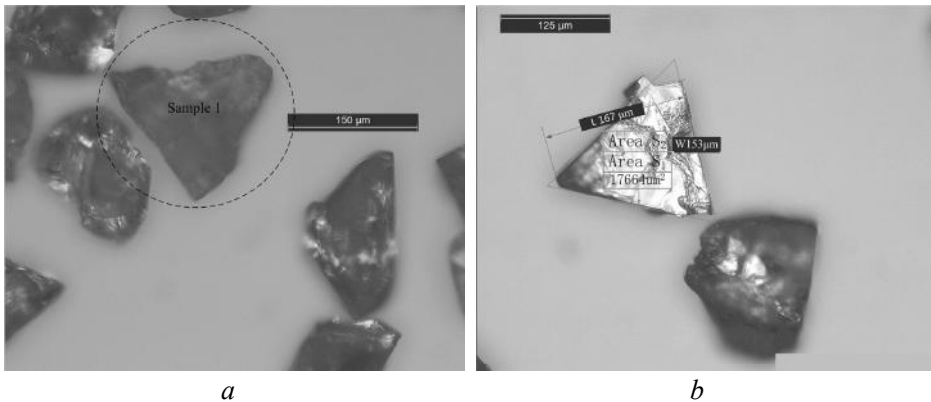Fig. 1. Sample group A with 5× magnification in full image (*a*), in enlarged image (*b*).

Fig. 2. Sample group B with 50× magnification in full image (*a*), in focusing image (*b*).

GRIT MORPHOLOGY CLASSIFICATION CRITERIA

Due to the lack of key volumetric information on 2D projection (matt or glossy), the microrelief of the particles with spatially volumetric features could be identified by utilising back light microscopy, surface division scanning technique on Bruker ContourGT platform (version 64) [21] and scanning electron microscopy (SEM) techniques. Combining with essential exposure highlight skills

(e.g. enhancing light intensity, hues, saturation and contrast and depth of measured field), some examples are shown in Fig. 4. The randomly captured geometry characteristics, including spiky apex, contour peaks, truncated profiles and prismatic columns, are visually extracted from top-surface/flanks inscribed with dotted lines or circles to determine dominant frustums and bases so as to dimension all samples edges according to calibration metrics and then calculate the ratio of top-surface area (S_1) to bottom-profile area (S_2) by conducting aforementioned quantitative dimension analysis of each grit edges. In contrast to many previous conclusions on 2D shape distribution determined by simple AR or circumscribed circle, a new categorisation method is proposed to classify the grits into four groups (e.g. ellipsoid, frustum pyramid, truncated cone and arbitrary polyhedron), six subgroups and eighteen subtypes of 3D characteristics categories. The identification criteria of categorisation are illustrated in Table 2 to identify and classify abrasive grits according to their geometries with acceptable similarity, uniqueness and practicability disregarding the broken or torn edges.
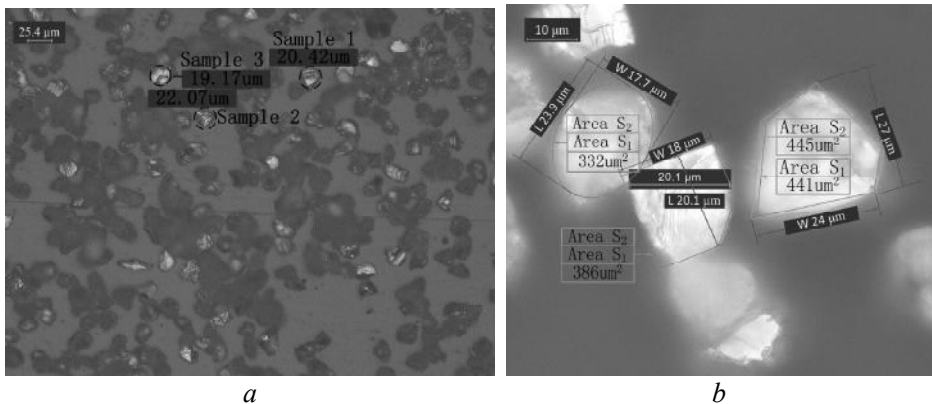

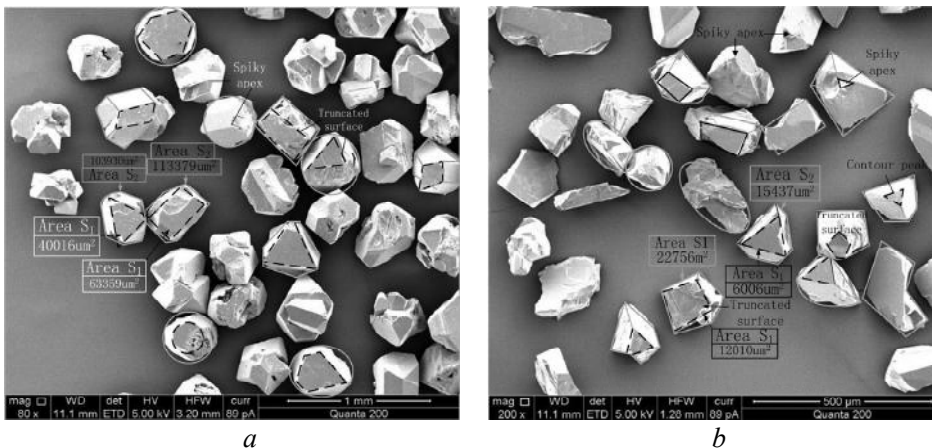Fig. 3. Sample group C with 10× magnification in full image (*a*), in enlarged image (*b*).

Fig. 4. SEM images group B (*a*), group C (*b*).

RESULT AND DISCUSSION
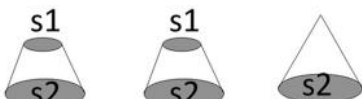
### Particle geometry and morphology distribution

Based on the classification methods defined in Table 2, the 3D morphological distributions of abrasive grits in groups A, B and C, whose sample numbers are

102, 159 and 133 respectively, are visually illustrated in Fig. 5 to Fig. 7 with histogram and pie charts to indicate the relationship between the sample amounts (in sub-histogram (*a*)) or morphology proportion (in sub-chart (*b*)) and relevant geometries. The geometrical shapes of each sample group are categorised with detailed sharp, broken and torn situations of particle edges are presented elaborately to facilitate the evaluation of quality control in milling and sieving processes and grinding performance. It can be seen that only a few types of geometrical shapes dominate the population of abrasive grits. Tetrahedron and pyramid shapes are among the most popular one.

Table 2. Morphology categorization criteria

Morphology categorization				Characteristics formulae	Projection disambiguatation
Group	Subgroup	Sub-type	Geometry		
			Sphere	$S1{:}S2 \geq 0.8$	None
			Ellipsoid	$S1{:}S2 < 0.8$	
		Triangular pyramid	$S1{:}S2 \leq 0.1$	Three edges and one highlighted peak
			Rectangular pyramid		Four edges and one highlighted peak
			Pentahedron		Five edges and one highlighted peak
			Rhombohedron		Six edges and one highlighted peak
			Frustum pyramid	$0.1 < S1{:}S2 < 0.8$	Three edges and one truncated top-surface
			Truncated tetrahedron		Four edges and one truncated top-surface
			Truncated pentahedron		Five edges and one truncated top-surface
			Truncated rhombohedron		Six edges and one truncated top-surface
		Triangular prism	$S1{:}S2 \geq 0.8$	Three edges and one truncated top-surface

Table 2. (Contd.)

Quadrangular prism		Four edges and one truncated top-surface
Pentahedral prism		Five edges and one truncated top-surface
Rhombohedral prism		Six edges and one truncated top-surface
Cone	S1:S2 ≤ 0.1	Round bottom-surface and one peak
Truncated cone	0.1 < S1:S2 < 0.8	Round bottom-surface and one top-surface
Cylinder	S1:S2 ≥ 0.8	Round bottom-surface and one top-surface
Arbitrary polyhedron	S1:S2 ≥ 0.8 or Number of edges > 6	Arbitrary poly-gon in top-surface

a *b*

Fig. 5. Morphology distribution of group A in histogram (*a*), in categorized pie charts (*b*).

a *b*

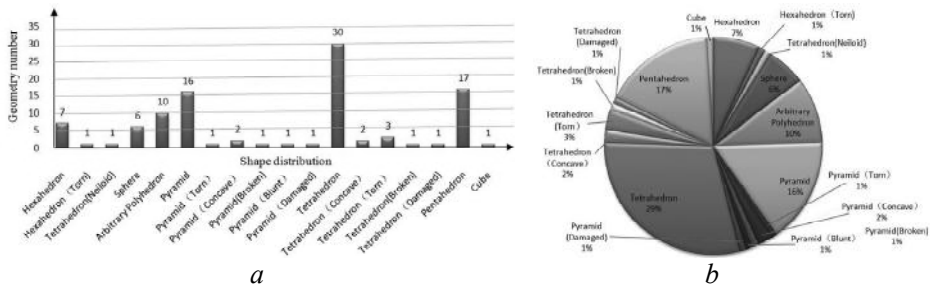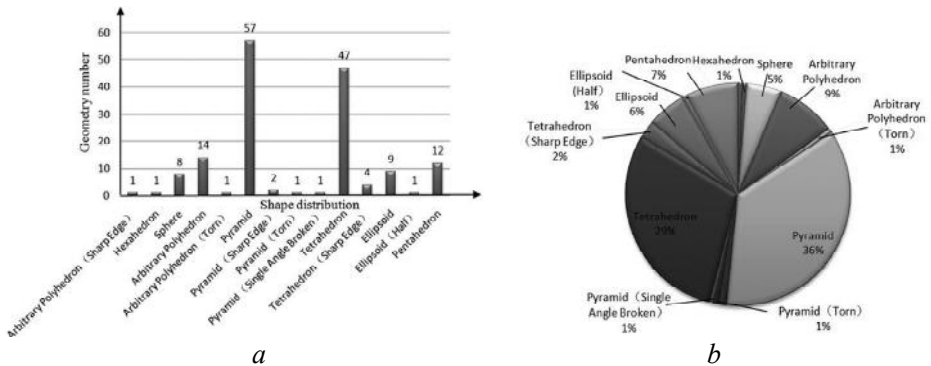Fig. 6. Morphology distribution of group B in histogram (*a*), in categorized pie charts (*b*).

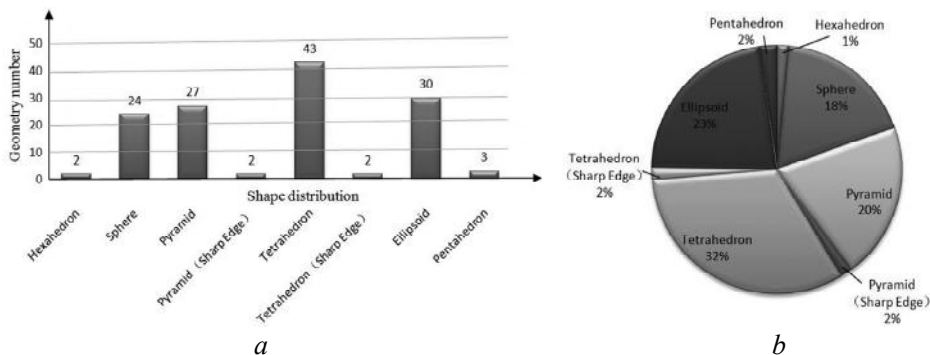*a*   *b*

Fig. 7. Morphology distribution of group C in histogram (*a*), in categorized pie charts (*b*).

Particle size and size distribution

The absolute values of maximum and mean in length and width bands and their size distribution of the samples are illustrated in Fig. 8. As an important index of morphological characteristics to indicate random distribution from measurement tests in industry, the variable x_i is defined as the AR of the width W_i to the length L_i of each abrasive grit, depicted as:

$$x_i = \frac{W_i}{L_i} .$$ (1)

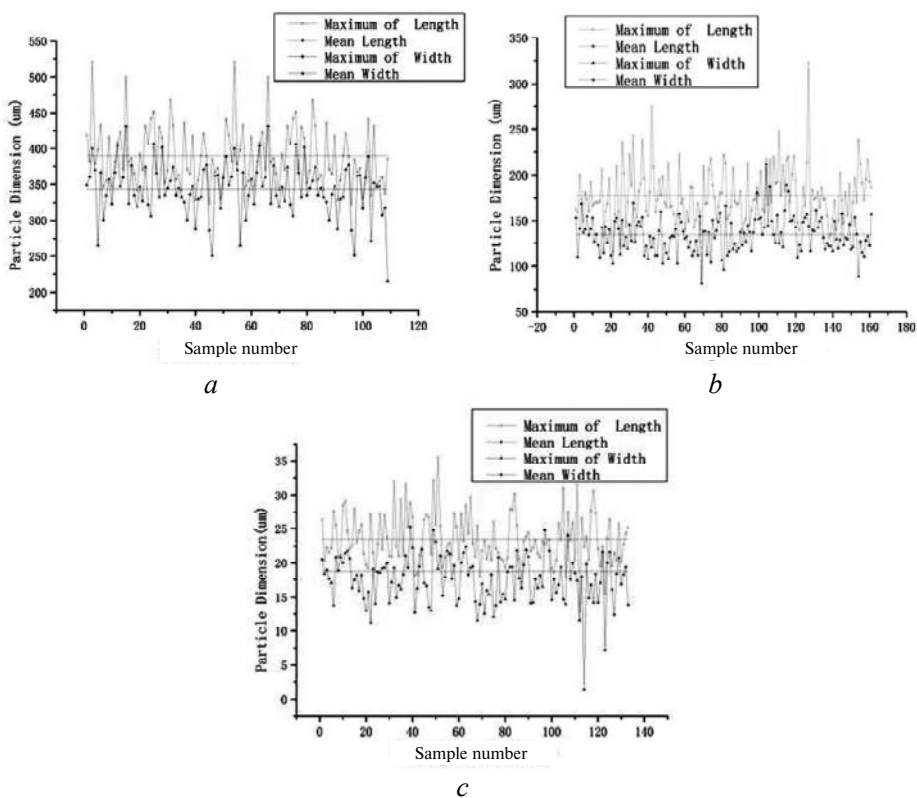*a*   *b*

c

Fig. 8. Size and size distribution of three samples group A (*a*), group B (*b*), group C (*c*): maximum of length (*1*), mean of length (*2*), maximum of width (*3*), mean of width (*4*).

The mean of AR is calculated as

$$\bar{x} = \sum_{i=1}^{n} \frac{x_i}{n},$$ (2)

where n is total number of the samples.

The standard deviation σ of size distribution of the width and length of the grits and their AR is defined to depict how all data of the grits sizes are spread out from the mean (the expected value), calculated by

$$\sigma = \sqrt{\sum_{i=1}^{n} \frac{(x_i - \bar{x})^2}{n}}.$$ (3)

The AR distribution of three groups of samples and their distribution density comparison diagram are shown in Fig. 9. By combining its size band with the standard deviation σ of the AR distribution, the shape and variation of abrasive distribution could be assessed for the conformance of production. The tighter the AR distribution of the grits in its size band, the greater the conformance of production is. The AR distribution of group A would be approximated as a Gaussian distribution which expected value is set to the mean of the AR and the probability density function is depicted as [22]

$$f(x) = \frac{1}{\sqrt{2\pi}\sigma} e^{\frac{-(x_i - \bar{x})^2}{2\sigma^2}}.$$ (4)

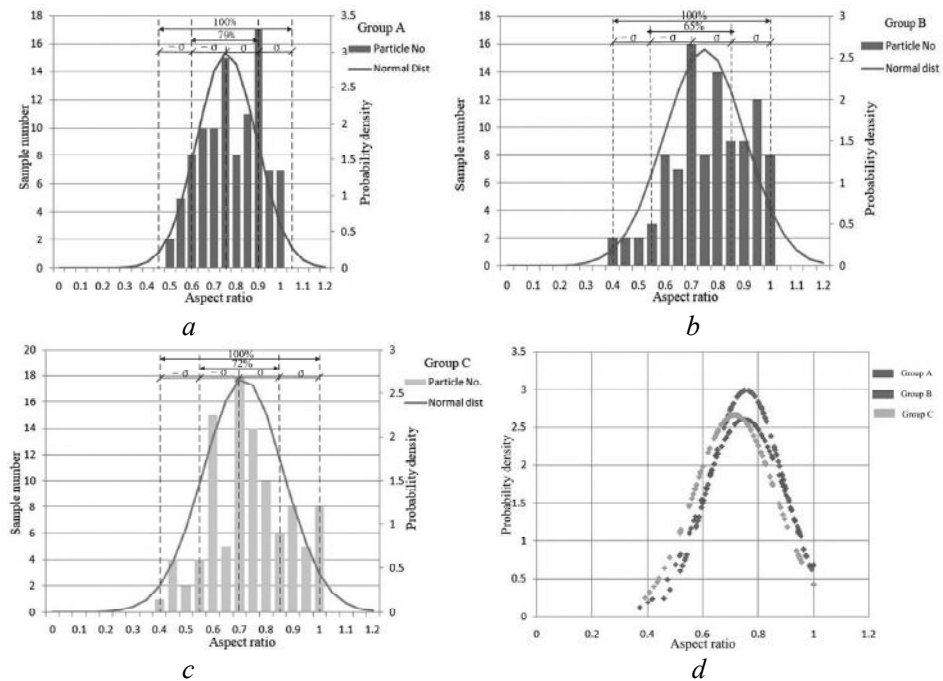Fig. 9. AR distribution of three samples group A (*a*), group B (*b*), group C (*c*), their resultant diagram (*d*).

With Gaussian distribution function, the results of group A in Fig. 9, *a* illustrate that the conformance of grit AR within $[\bar{x} - \sigma, \bar{x} + \sigma]$ is 79 % (empirical reference value in industry is 68.3 %) and within $[\bar{x} - 2\sigma, \bar{x} + 2\sigma]$ is 100 % (empirical refer-

ence value is 95.4 %) respectively [23]. The similar analysis results are observed in Figs. 9, *b* and *c*.

Moreover, as illustrated in Fig. 9, *d*, the bigger σ, the wider the AR values scatter (e.g. group B) and the greater the random variation. However, the narrower distribution of the AR values (e.g. group A) does not necessarily lead to less variation of the morphological geometries within the size band of the grits. In fact, the Group A presents more morphological types of grits than other groups. Although the conformance proportion of abrasive grits size and AR values could reveal quality satisfaction of abrasive production, it does not reveal the abrasive grit shape variation. This convinces that 3D morphological features are necessary to provide a rational guidance to improve core competency for abrasive tool manufacturers and users.

Morphology analysis and its significance

Combined with all data from Fig. 5 to Fig. 9, the properties and geometry characteristics of all studies samples that are interested for different stakeholders are summarized in Table 3.

Table 3. Comparison of geometry, size and their distribution of all samples

Sample types	Group A	Group B	Group C
Particle scale	Coarse micron	Finer micron	Sub-sieving powder
Dominant geometries and proportion	Tetrahedron, 29 %	Pyramid, 36 %	Tetrahedron, 32 %
	Pentahedron, 17 %	Tetrahedron, 29 %	Ellipsoid, 23 %
	Pyramid, 16 %	Arbitrary polyhedron, 9 %	Pyramid, 20 %
	Arbitrary polyhedron, 10 %	Pentahedron, 7 %	Sphere, 18 %
Mean of length, μm	390.5	178	23.5
Standard deviation of length (σ)	43.8	24.56	3.92
Size range of dimensioned length and conformance proportion within $[\bar{x}-\sigma, \bar{x}+\sigma]$	[354, 438] 72 %	[140, 200] 77 %	[18, 27] 73 %
Mean of width, μm	343.3	134	18.7
Standard deviation of width σ	35.7	19.2	3.21
Size range of dimensioned width and conformance proportion within $[\bar{x}-\sigma, \bar{x}+\sigma]$	[304, 378] 79 %	[101, 152] 65 %	[13, 20] 72 %
Mean of AR of width/length	0.76	0.75	0.71
Probability density of AR	2.98	2.6	2.66
Sieving mesh size, μm (ANSI-B74-16)	[302, 456]	[127, 165]	[12, 22]

In Table 3, the particles of group A in coarse micron scale have a mean value of width (343.3 µm) close to the low limit of sieving mesh size standard ([302, 456] µm) (Reference: ANSI-B74-16 [19]) and a size range ([304, 378] µm) with highest conformance proportion (79 %) in three samples. It demonstrates the validation of measurement results [23] but unsatisfying level of milling and sieving in the pre-process, which makes comparatively smaller particles than required standard ones around sieving mesh size. Moreover, the arbitrary polyhedron with great proportion of 10 % of the samples also confirms the unsatisfying situation. The pre-process should be improved to obtain satisfying shape (with consistent features of dominant grit shapes) and size band (around the mean of standard size range) of the particle in the future. The real dominant geometries of the particle are tetrahedron, pentahedron and pyramid in proportion order, as shown in Fig. 5, even though internal features, e.g. cutting edges companying with irregular broken, torn and sharp are observed in captured images. It is essential for researchers by taking tetrahedron or pentahedron geometrical shapes as key features in modelling group A grit performance and to conduct dynamics signals monitoring and simulation and further to predict grinding performance, friction and wear behaviour of abrasive tools [16, 24].

The particles of group B, as finer micron grits, have a mean value of width (134 µm) close to the low limit of sieving mesh size standard ([127, 165] µm) shows a wider size distribution band ([101, 152] µm) but the lowest conformance proportion of width band of 65 % (less than 68.3 %). It demonstrates that a certain proportion of tiny or over-sized grits with wider distribution band shown in Fig. 9, *b* and a diverse morphology distribution (e.g. arbitrary polyhedron, irregular sphere and ellipsoid with shattered edges, etc) blended with of the dominant geometries of the particle, which cause the measurement difficulty on exactly morphology identification. The dominant geometries of the particles are pyramid and regular tetrahedron (the sum of two proportions is 65 %), as shown in Fig. 6. Thus, these two geometries should be approximately considered in modelling the simplified geometry for simulating chip formation, dynamic friction and wear behaviour. Furthermore, a large number of grit geometries with shattered edges and irregular morphology distribution make it more complex in abrasive tool preparation for designated pattern and grinding dynamics prediction. During grinding ductile materials (e.g. copper), because the different shapes of micro-cutting edges (i.e. circular/square/triangular base frustums) would influence the grinding performance (e.g. shearing/fracturing/plastic deformation, surface texture, surface roughness, specific cutting forces), the increased number of cutting edges on grits could produce more localised material pile-up and reduce plastic chip removals [2, 3, 16]. Moreover, the shearing/fracturing phenomena were preponderant in the material removal mechanism when using square/triangular shaped grits while major plastic deformations were found for circular base frustum during grinding brittle materials (e.g. sapphire or ceramics) [16]. The sharp cutting edges of single grit, as shown in Fig. 2, would easily result in grit fracture, crack propagations and re-sharpening during grinding process even though the git material is of high strength and thermal stability, which are beneficial to achieve finish ground surface.

The particles of group C, as a sub-sieving powder, which mean value of width (18.7 µm) is closer to the upper limit of sieving mesh size standard ([12, 22] µm) than the other two particles, have a tighter size band ([13, 20] µm) as shown in Fig. 8, *c*. This is the evidence that the high quality control of milling, sieving and sedimentation techniques has been implemented in pre-process procedure. The

morphology distribution of the particle mainly composes of tetrahedron and ellipsoid with high proportion (the sum of two proportions is 55 %), accompanying with pyramid and sphere at high proportion as well. The proper mean of AR (0.71) as shown in Fig. 9, *c*, is ideal and optimal for practical manufacture process to improve the holding force distribution of the diamond abrasives [5, 6]. Meanwhile, most of the grits with bulky and unbroken edges, which induce block shear behaviour, are beneficial to achieve smoother workpiece surface roughness, less clogging and abrasive grit wear. This results in predominantly bulk material displacement or plastic deformation in orthogonally orientated working-surface when machining difficult-to-machine ductile materials with high hardness at high and super-high speed [16, 25, 26].

CONCLUSIONS

Through high quality control in pre-process and pro-process procedures, abrasive grits at a tight size band and high forming accuracy remains one of the most important influence factors on abrasive grinding/polishing tools preparation, removal mechanism and grinding performance. Because particle-sorting techniques and quality-evaluating system are often accompanied with special device, microscopy techniques and comprehensive identification criteria with low efficiency and high cost, they are seldom openly discussed. It is widely required among grit providers, abrasive machining tool manufacturer and user to have scientific insight on the identification and morphology categorization of spatially volumetric geometry and size distribution of abrasive grits in micron scale.

For this purpose, a new categorisation method is proposed to enable the size and morphological distribution of volumetric geometries of abrasives to be standardised for grinding dynamics analysis and simulation, which is beneficial to grinding performance prediction. By means of conducting microscopy measurement tests, three types of abrasive grits were assessed in terms of the aspect ratio of width to length of the samples, dominant volumetric shapes, tight size distribution, their standard deviation and conformance proportion. It is found that only a few types of grit morphologic geometries dominate the grit population. After the analysis of current methods used in abrasive machining research, it is suggested that the analysis of abrasive processing should focus on a set of dominant grit shapes rather than just single simplified geometry. With the observation and analysis, the dominant volumetric geometries of grits are tetrahedron and pentahedron for sample group A, tetrahedron and ellipsoid for sample group B and geometries of pyramid and tetrahedron for sample group C.

FUNDING

Характеристика розподілу геометричної форми та розміру абразивних зерен з високою якістю у щільному діапазоні розмірів і точна картина є вирішальною для сучасного виробника інструменту для виготовлення абразивного інструменту з дрібнодисперсного порошку та інших порошкових інструментів, складних для класифікації та оцінки з огляду на відсутність наукового методу. На відміну від промислових методів класифікації по розмірам сітчастих комірок або спрощених критеріїв проекції з обмеженим (вписаним або описаним) колом або прямокутником, розроблено та затверджено набір нових системних критеріїв шляхом вимірювання трьох репрезентативних зразків зерен в мікронній шкалі під 2D/3D мікроскопією. До особливостей мікронних абразивних зерен за морфологічною класифікацією належать чотири групи, шість підгруп та

вісімнадцять підтипів з урахуванням просторової геометрії та статистичного розподілу розмірів. Для аналізу та моделювання продуктивності шліфування було б краще використовувати набір домінуючих об'ємних геометрій, а не використовувати одну просту геометрію. Крім того, обговорюється значення геометрії абразивних зерен при шліфуванні.

Ключові слова: *суперабразивний порошок, морфологічний аналіз, категоризація характеристик, техніка мікроскопії; розподіл розмірів.*

Характеристика распределения геометрической формы и размера абразивных зерен с высоким качеством в плотном диапазоне размеров и точная картина является решающим для современного производителя инструмента для изготовления абразивного инструмента из мелкодиспетного порошка и других порошковых инструментов, сложных для классификации и оценки, учитывая отсутствие научного метода. В отличие от промышленных методов классификации по размерам сетчатых ячеек или упрощенных критериев проекции с ограниченным (вписанным или описанным) кругом или прямоугольником, разработан и утвержден набор новых системных критериев путем измерения трех репрезентативных образцов зерен в микронной шкале под 2D/3D микроскопией. К особенностям микронных абразивных зерен по морфологической классификации относятся четыре группы, шесть подгрупп и восемнадцать подтипов с учетом пространственной геометрии и статистического распределения размеров. Для анализа и моделирования производительности шлифования было бы лучше использовать набор доминирующих объемных геометрий, а не использовать одну простую геометрию. Кроме того, обсуждается значение геометрии абразивных зерен при шлифовании.

Ключевые слова: *суперабразивний порошок, морфологический анализ, категоризация характеристик, техника микроскопии; распределение размеров.*

1. Darafon A., Warkentin A., Bauer R. 3D metal removal simulation to determine uncut chip thickness, contact length and surface finish in grinding. *Int. J. Adv. Manuf. Technol*. 2013. Vol. 66, no. 9–12. P. 1715–1724.
2. Aurich J.C., Kirsch B. Kinematic simulation of high-performance grinding for analysis of chip parameters of single grits. *CIRP Ann. Manuf. Sci. Technol*. 2012. Vol. 5, no. 3. P. 164–174.
3. Rasim M., Mattfeld P., Klocke F. Analysis of the grit shape influence on the chip formation in grinding. *J. Mater. Proc. Technol*. 2015. Vol. 226, no. 9. P. 60–68.
4. Chen Y., Huang G.Q. Development and research on the dynamics simulation system for surface grinding process with diamond wheel. *Key Eng. Mater*. 2014. Vol. 589–590. P. 658–664.
5. Li X.K., Wolf S., Zhu T.X., Geng Z., Rong Y.M. Modelling and analysis of the bonding mechanism of CBN grit for electroplated superabrasive tools–part 2: finite element modeling and experimental verification. *Int. J. Adv. Manuf. Technol*. 2015. Vol. 77, no. 1–4. P. 43–49.
6. Fu Y.C., Tian L., Xu J.H., Yang L. Development and application on the grinding process modelling and simulation. *J. Mechan. Eng*. 2015. Vol. 51, no. 7. P. 198–205.
7. Benea I.C. Particle size and size distribution of superabrasive powders. Diam. Tooling J. 2010. Vol. 10, no. 3. P. 39–46.
8. List E., Frenzel J., Vollstadt H. A new system for single particle strength testing of grinding powder. *Ind. Diam. Rev*. 2006. Vol. 66, no. 1. P. 42–47.
9. Petasyuk G.A. System and criterial method of the identification and quantitative estimation of the geometrical shape of the abrasive powder grit projection. *Powder Technol*. 2014. Vol. 264. P.78–85.
10. Agata S., Pawel Z., Andrzej B. Selection of shape parameters that differentiate sand grits based on the automatic analysis of two-dimensional images. *Sedi. Geo*. 2015. Vol. 327, no. 70. P. 14–20.
11. Mahamed G.H., Ayed S., Engellbrecht A.P. Dynamic clustering using particle swarm optimization with application in image segmentation. *Pat. Analysis Appl*. 2006. Vol. 8, no. 4. P. 332–344.
12. Igathinathane C., Pordesimo L.O., Columbus E.P. Shape identification and particle size distribution from basic shape parameters using Image L. *Comput. Electron. Agric*. 2008. Vol. 63, no. 2. P. 168–182.
13. Kröner S., Doménech-Carbŏ M.T. Determination of minimum pixel resolution for shape analysis: proposal of a new data validation method for computerized images. *Powder Technol*. 2013. Vol. 245, no. 8. P. 297–313.

14. Aurich J.C., Herzenstiel P., Sudermann H., Magg T. High-performance dry grinding using a grinding wheel with a defined grit pattern. *CIRP Ann. Manuf. Technol*. 2008. Vol. 57, no. 1. P. 357–362.

15. Herzenstiel P., Aurich J.C. CBN-grinding wheel with a defined grit pattern – extensive numerical and experimental studies. *Mach. Sci. Technol*. 2010. Vol. 14, no. 3. P. 301–322.

16. Axinte D., Butler-Smith P., Akgun C., Kolluru K. On the influence of single grit microgeometry on grinding behaviour of ductile and brittle materials. *Int. J. Mach. Tools Manuf*. 2013. Vol. 74, no. 8. P. 12–18.

17. Koshy P., Iwasaki A., Elbestawi M.A. Surface generation with engineered diamond grinding wheels: insights from simulation. *CIRP Ann. Manuf. Technol*. 2003. Vol. 52, no. 1. P. 271–282.

18. Linke B.S. A review on properties of abrasive grits and grit selection. *Int. J. Abra. Technol*. 2015. Vol. 7, no. 1. P. 46–58.

19. American National Standard Institute (1992) Norm ANSI B74.4-1992: Procedure for Bulk Density of Abrasive Grain. Nov. 12. 1992.

20. Leica Application Suite (LAS) Handbook (2010) [online] http:// www.leica-microsystems.com. Solms, Germany.

21. Bruker Handbook Measurement and Characterization of Surface Topography. Bruker cooperation. Karlsruhe, Germany, 2012.

22. Soong T.T. Probability and Statistics for Engineers and Scientists. Chichester: John Wiley&Sons, 2004.

23. Liang C.C., Li R., Shi X.W. A compact closed form of standard normal distribution. *J. Xidian. Univ*. 2003. Vol. 4(3). P. 289–292 (in Chinese).

24. Pirard E. The cutting edge of superabrasives quality control. *Ind. Diam. Rev*. 2003. Vol. 3, no. 3. P. 49–50

25. Malkin S., Guo C. Grinding Technology: Theory and Application of Machining with Abrasives. New York: Industry Press, 2008.

26. Doman D.A., Warkentin A., Bauer B. A survey of recent grinding wheel topography models. *Int. J. Mach. Tools Manuf*. 2006. Vol. 46, no. 3–4. P. 343–352.